ISSN 1990-7931, Russian Journal of Physical Chemistry B, 2021, Vol. 15, No. 6, pp. 1072–1083. © The Author(s), 2021. This article is an open access publication.
ISSN 1990-7931, Russian Journal of Physical Chemistry B, 2021. © The Author(s), 2021. This article is an open access publication.
Russian Text © The Author(s), 2021, published in Khimicheskaya Fizika, 2021, Vol. 40, No. 11, pp. 65–77.

CHEMICAL PHYSICS OF NANOMATERIALS

Effect of Composition and Structure of Metal Oxide Composites Nanostructured on Their Conductive and Sensory Properties

G. N. Gerasimov[a], V. F. Gromov[a], M. I. Ikim[a, *], and L. I. Trakhtenberg[a, b]

[a] *Semenov Federal Research Center for Chemical Physics, Russian Academy of Sciences, Moscow, Russia*

[b] *Moscow State University, Moscow, Russia*

**e-mail: ikim1104@rambler.ru*

Received April 28, 2021; revised May 14, 2021; accepted May 20, 2021

Abstract—The relationship between the structure and properties of nanoscale conductometric sensors based on binary mixtures of metal oxides in the detection of reducing gases in the environment is considered. The sensory effect in such systems is determined by the chemisorption of oxygen molecules and the detected gas on the surface of metal oxide catalytically active particles, the transfer of the reaction products to electron-rich nanoparticles, and subsequent reactions. Particular attention is paid to the doping of nanoparticles of the sensitive layer. In particular, the effect of doping on the concentration of oxygen vacancies, the activity of oxygen centers, and the adsorption properties of nanoparticles is discussed. In addition, the role of heterogeneous contacts is analyzed.

Keywords: conductometric sensor, nanoscale structured metal oxides, doping, electronic and chemical sensitization, reducing gases

DOI: 10.1134/S1990793121060038

INTRODUCTION

The main qualities that sensors used in various fields should have are sensitivity to analytes even at their concentration at the ppb level, speed, and stability. At present, the most widely used conductometric chemical sensors that meet these requirements are those using semiconductor metal oxides with nanosized crystals as a sensitive layer. Such sensors are reliable and easy to manufacture and are used both in everyday life and in production for monitoring the environment, in medicine, and in other applications, in particular for the detection of ammonia at refrigeration plants, methane in mines, and carbon monoxide in exhaust gases [1–3]. Their small size and relatively low cost allow them to be used also as personal sensors.

Work on the creation of conductometric chemical sensors began in the 1950s–1960s, when it was shown that at temperatures of ~400°C metal oxides change their resistivity when exposed to various chemical compounds (see, for example, review [4], where these articles are cited). Soon thereafter, sensory devices such as the Taguchi sensors based on tin oxide appeared [5]. Subsequently, work in this direction was mainly devoted to expanding the range of metal oxide systems with sensory properties and elucidating the peculiarities of the mechanism of action of these systems (a discussion of works in this direction is presented, in particular, in reviews [3, 6, 7]).

The detection of reducing compounds by metal oxide sensors is based on the fact that their sensitive layer contains chemisorbed oxygen, which captures electrons from the conduction band of semiconductor nanoparticles. At the same time, oxygen anionic centers such as O^-, O^{2-}, and O_2^- can form on the surface of these particles. The structure and concentration of the oxygen centers depends on the chemisorption temperature [8, 9].

Taking into account the currently accepted model of the sensory process in the detection of reducing compounds, it can be assumed that the sensory effect is determined by two processes: the adsorption of the analyzed compounds and oxygen on the surface of the metal oxide sensor particles and the reaction of the adsorbed compounds with oxygen centers O^- on this surface. The main disadvantage of single-component semiconductor sensors is their low selectivity for detecting compounds of the same type, in particular, various reducing gases. At the same time, the selectivity and the sensitivity of conductometric sensors are improved when using multicomponent composite systems that combine metal oxides with different electronic characteristics and chemical properties (see, for example, [10–15]). In this case, we should distinguish

between the introduction of low concentrations of doping oxides [10, 15, 16] and the situation when their commensurate concentrations are used [11, 17–20]. In the second case, some works were carried out with a targeted combination of nanoparticles in comparable concentrations of an electron-rich oxide (In_2O_3) and catalytically active SnO_2 [18], ZnO [19], and CeO_2 [20]. This combination turned out to be very productive and the sensitivity of the sensor increased significantly. In [21–25], a noticeable effect of the composition on the conducting properties of the composite was noted.

At present, a great deal of attention is paid to the development and study of binary metal oxide sensor systems structured at the nanoscale, especially since conductometric semiconductor sensors consisting of metal oxide crystalline nanoparticles are the most common means of detecting various impurities in the atmosphere. The sensory effect in the detection of reducing gases in the systems under consideration structured at the nanoscale depends on two factors [26, 27]. The first one (receptor function) is the chemisorption of the detected gas and oxygen on the surface of individual metal oxide particles, which is determined by the physicochemical properties of the particles, and the subsequent interaction of the chemisorbed gas with the oxygen centers (sensory reaction). The second factor (transducer function) is the transformation of the electronic state of particles, which occurs as a result of a sensory reaction, which leads to a change in the conductivity of the sensitive layer. In a mixed metal oxide system consisting of components with different electronic and physicochemical properties, both factors of the sensory process depend on the interaction between the components, which opens up additional opportunities for increasing the efficiency of the sensory system.

Let us discuss what types of interactions are realized in mixed oxide systems. The overwhelming majority of metal oxides are ionic compounds; therefore, the transition of the metal ions of one component into nanoparticles of another is possible in the composite (doping of nanoparticles). This doping occurs mainly during the synthesis of nanosized crystals of the composite and leads to a change in the structure and properties of nanoparticles.

In addition, we should take into account the contacts between semiconductor nanoparticles of various sizes and electronic structures, leading, in particular, to the transfer of electrons between particles and the mutual charging of the contacting nanoparticles [28, 29]. Under the conditions of the interaction of the sensor with the molecules of the analyzed gas, the transfer of chemisorbed molecules and the products of their reactions with metal oxide (in particular, active products such as atoms or radicals) between the contacting nanoparticles of the components (spillover) is also possible. Of course, the separation of composites by the type of interaction between components is conditional, since a change in the structure of nanoparticles due to the doping of one metal oxide composite with ions of another component can significantly affect the processes occurring during contacts of nanoparticles.

Note that the description of the sensory effect is largely based on the distribution of electrons in semiconductor nanoparticles [12, 30]. In this case, it is also necessary to take into account the various mechanisms of interaction of nanoparticles [31]. As for the sensory effect, its theory in one-component systems was developed in [32–34]. A comparison with the experimental data is also given there.

The review considers the interaction between the components of semiconductor composites structured at the nanoscale depending on the structure and chemical properties of metal oxides, as well as on the method of their formation. The primary attention is paid to the influence of this interaction on the chemical processes that determine the operational properties of composite sensors to detect reducing gases in the atmosphere.

STRUCTURE OF PARTICLES IN COMPOSITES

The interaction of the components of a binary metal oxide system can lead to the incorporation of cations of one metal oxide into crystalline nanoparticles of another component (doping). As a result, ions are replaced in the lattice of particles with the formation of a corresponding solid solution, which ultimately can have a significant effect on the sensory properties of the composite. This is observed during the formation of composites during the codeposition of components from solutions containing a mixture of salts or organometallic precursors [14], as well as when crystals of one metal oxide are impregnated with a solution of a salt of another metal, followed by heat treatment of the impregnated samples [10, 35].

The effect of this substitution of ions in crystalline metal oxide nanoparticles on their properties depends on the size and valence of the metal ions. A distinction is made between isovalent doping, in which the valences of the main ions that make up the crystal lattice and the doping ions are the same, and heterovalent doping, when the valences of the metals are different.

Isovalent Doping

With isovalent doping, changes in the structure and properties of particles are caused by the deformations of bonds in the lattice when the main ions of the lattice are replaced by doping ions of the same charge, but of a different size and with different electronic characteristics. The energy of ionic bonds in the lattice of a metal oxide crystal, E_{MO}, depends on the surface charge density of the metal cations in the lattice and increases with a decrease in the size of the cations.

Thus, the quantity E_{MO} increases as a result of the compression of the crystal lattice observed upon partial (in the concentration range 0–15 wt %) substitution of In^{3+} ions (radius 0.80 Å) by the smaller Al^{3+} (radius 0.54 Å) during the formation of the In_2O_3–Al_2O_3 composite [36]. This leads to a decrease in the total concentration of oxygen vacancies in the bulk and on the surface and, accordingly, in conduction electrons in nanocrystals of the composite [37]. It was found by photoluminescence that the concentration of oxygen vacancies also decreases as a result of the compression of the lattice of SnO_2 nanocrystals when doped with Ti^{4+} ions (radius 0.64 Å) [38]. At the same time, decrease in E_{MO} as a result of lattice expansion upon the replacement of 5% In ions^{3+} by larger La ions^{3+} (radius 1.03 Å) in La_2O_3–In_2O_3 composites [39, 40] is accompanied by an increase in the concentration of oxygen vacancies [41] and an increase in the conductivity of the composite [42].

According to X-ray photoelectron spectroscopy (XPS) data, when doping ions such as Al^{3+} and La^{3+} into In_2O_3 nanocrystals, the content of the chemisorbed oxygen on the surface of these nanocrystals increases [36, 39, 40, 42]. This indicates an increase in the number of oxygen chemisorption centers, which are surface oxygen vacancies. Vacancies contain metal ions that are not fully coordinated with the oxygen ions of the metal oxide lattice and therefore have an increased affinity for oxygen molecules and other agents in the gas phase. The chemisorption of oxygen molecules on oxygen vacancies leads to the dissociation of O_2 and the formation of radical anions O^- [43], which are the active centers of the sensory response.

It is interesting that the number of surface oxygen vacancies in In_2O_3 nanocrystals doped with Al ions^{3+} increases in all cases of substitution of the main lattice ions, even with a decrease in the total number of vacancies [36]. This can apparently be explained by the differences in the structures of the surface layer and deeper layers of the crystal.

Indeed, the incorporation of smaller ions leads not only to lattice compression and a decrease in the number of vacancies in relatively deep layers of the nanocrystal but also to the additional disturbance of the surface structure and, accordingly, to an increase in the number of surface vacancies. In the case of the incorporation of larger ions, the number of vacancies increases both in the volume and on the surface. Consequently, with any violation of the regularity of the structure of a nanosized object, the concentration of active centers on the surface, and with it the sensitivity of the sensor, will increase.

The increase in the content of chemisorbed oxygen on the surface of In_2O_3 nanocrystals caused by their isovalent doping with Al^{3+} and La^{3+} ions, leads to an increase in the sensory effect in the detection of various reducing gases, especially hydrogen sulfide and oxygen-containing organic compounds (formaldehyde, ethanol, acetone, etc.) [36, 39, 40, 42]. The increased sensory effect during the detection of compounds of this nature also occurs as a result of isovalent doping of SnO_2 with Ti^{4+} [44, 45].

Heterovalent Doping

Despite the change in the sensory effect observed upon isovalent doping, the primary attention of researchers is focused on the heterovalent doping of metal oxide nanocrystals, which is much more effective for increasing the sensitivity and selectivity of sensors. In this case, during the formation of composites, the ions of one metal oxide component passing into nanoparticles of the other cause a redistribution of charges related to the movement of ions between the components of the composite.

The formation and disappearance of oxygen vacancies upon heterovalent substitution of Sn ions^{4+} by Sb^{5+} ions during the formation of the SnO_2–Sb_2O_5 composite from solutions of tin and antimony salts leads to an increase in the conductivity of the composite in comparison with SnO_2 [46]. This process is described by the equation

$$Sb_2O_5 + 2Sn_{Sn} \leftrightarrow 2Sb^+_{Sn} + 2e^- + 0.5O_2 + 2SnO_2, \quad (1)$$

where Sn_{Sn} and Sb^+_{Sn} are Sn^{4+} and Sb^{5+}ions in the SnO_2 lattice, and e^- are SnO_2 conduction electrons compensating the positive charge of the centers Sb^+_{Sn}. The Sb^{5+} ion substituting the Sn^{4+} ion in the lattice, forms a donor level near the conduction band of SnO_2 [46]. The increase in conductivity in this system is explained by the appearance in it of additional electron-donor centers Sb^+_{Sn}, which increases the concentration of the conduction electrons.

The same phenomenon occurs as a result of the substitution of In^{3+} in Sn^{4+} and the formation of donor centers Sn^+_{In} in the In_2O_3 crystals upon the dissolution of SnO_2 in In_2O_3 [35, 47]. Note that in the X-ray diffractometry (XRD) spectra of the SnO_2–In_2O_3composites, obtained by impregnation and containing from 5 to 20 wt % SnO_2, only peaks related to nanoparticles and nanosized clusters of In_2O_3 are observed. There are no peaks corresponding to tin oxide. This means that the SnO_2 molecules do not form a noticeable number of individual nanoclusters, but mainly dissolve in nanosized In_2O_3 objects. The indium oxide crystals are surrounded by small crystalline In_2O_3 nanoparticles of 7 nm, which are formed on the surface of larger In_2O_3 crystals in the case of violations of their surface during the impregnation process.

The Sn^{4+} ions dissolve in small amounts in In_2O_3 crystals while expanding the In_2O_3 lattice due to the

appearance of an additional positive charge of the tin ion [35]. In this case, additional electrons, as in (1), are released and pass into the conduction band. With an increase in the concentration of SnO_2 the conductivity of the system increases to its maximum concentration of 5 to 7 wt %, which in this case, during the formation of SnO_2–In_2O_3 by the impregnation method corresponds to the maximum solubility of SnO_2 in In_2O_3 nanoparticles. When the content in the composite is more than 7% SnO_2 the conductivity begins to decrease, which can be explained by the formation of clusters of tin oxide with a higher electron affinity than that of In_2O_3 nanocrystals capturing In_2O_3 conduction electrons. As in other binary composites obtained from solutions, such clusters are not detected in the XRD spectra due to their small size.

It should be noted that both in the SnO_2–Sb_2O_5 system [48] and in the SnO_2–In_2O_3 system [35, 47] observed at low concentrations of SnO_2 an increase in conductivity is accompanied by a decrease in the sensory response. This is due to a decrease in the concentration of oxygen vacancies, which serve as centers of oxygen chemisorption with the formation of active oxygen O^- anions involved in sensory reactions [35, 43, 49, 50].

The replacement of metal oxide crystal cations with lower valence metal ions, on the contrary, leads to an increase in the number of oxygen vacancies and a decrease in the conductivity of the composite, as a result of which an increase in the sensory effect occurs. A typical example is the dissolution of In_2O_3 in SnO_2 nanocrystals when forming SnO_2–In_2O_3 composites in the process of the codeposition of these oxides from aqueous solutions of tin and indium salts [46] or impregnation of In_2O_3 crystals by solutions of tin salts [35]. In the latter case, In ions are transferred to SnO_2 nanoclusters during their growth on the surface of In_2O_3 matrix crystals. Incorporation of the In^{3+} ion into a tin oxide lattice that is larger than the tin ion leads to an increase in the interplanar distance $d(110)$ in SnO_2 [35].

Replacement of Sn ions by In ions in the SnO_2 lattice proceeds as follows [46]:

$$In_2O_3 + 2Sn_{Sn} + O_O \leftrightarrow 2In'_{Sn} + V_O^{++} + 2SnO_2, \quad (2)$$

where Sn_{Sn} and O_o are Sn^{4+} and O^{2-} ions in the SnO_2 lattice, In'_{Sn} is the In^{3+} ion replacing Sn^{4+} in the SnO_2 lattice and creating a localized negative charge in it, and V_O^{++} is a double positively charged oxygen vacancy.

It was established in [35] that the maximum increase in the interplanar distance $d(110)$ SnO_2 in the 40% SnO_2–60% In_2O_3 composite caused by the substitution of indium ions by tin ions and leading, according to (2), to the formation of additional oxygen vacancies in the SnO_2 lattice, corresponds to the maximum sensory response of 1400 to the presence of hydrogen.

Thus, upon the dissolution of In_2O_3 in SnO_2 nanocrystals, acceptor centers In'_{Sn} and an additional number of oxygen vacancies V_O^{++} are created in them. This leads to an increase in the oxygen chemisorption and an increase in the sensory effect in the detection of reducing compounds. Similar complexes of doping cobalt ions and SnO_2 oxygen vacancies, forming centers of oxygen chemisorption on the surface of SnO_2 nanocrystals, are described and discussed in [51].

An increase in the sensory effect was also noted upon the detection of CO by nanocrystalline SnO_2 doped with Ni^{3+} and Zn^{2+} ions, which replaced the Sn^{4+} ions in the SnO_2 lattice [52]. It was shown in [53] that an increase in the content of oxygen vacancies and, accordingly, chemisorbed oxygen causes an increase in the sensory effect upon detection of CH_4 by SnO_2 nanocrystals containing Cr^{3+} ions in the lattice. The doping of SnO_2 by Eu^{3+} ions also leads to sensitization of the sensory effect during the detection of acetone [54].

Effect of Doping on the Position of the Fermi Level

The relationship between the magnitude of the sensor effect and the electronic structure of the metal oxide sensitive layer was studied in detail by doping indium oxide nanocrystals with ions of various metals [55, 56]. It was found that the effect of ions dissolved in the lattice of In_2O_3 nanocrystals on the sensory effect is determined by the action of these ions on the position of the Fermi level (E_F). It turned out that the E_F of In_2O_3 nanocrystals increases with doping with Al, Ga, and Zr ions. For example, an increase in the Fermi level upon doping with In_2O_3 with aluminum is confirmed by measuring the work function by the Kelvin scanning probe method. Thus, the work function for pure In_2O_3 is 4.99 eV, which is higher than for the composite containing 15 wt % Al_2O_3 (4.85 eV) [57].

An increase in the Fermi level of nanocrystals doped with Al, Ga, and Zr ions causes an increase in the concentration of oxygen chemisorbed on the crystal surface and, accordingly, an increase in the sensory effect; and a decrease in E_F upon doping with Ti, Sn, Cr, W, and V ions, causes a decrease in the sensory effect [55]. Meanwhile, it was found that when detecting reducing gases with an aluminum-doped indium oxide sensor, the effect of aluminum on the sensory effect depends on the reducing ability of the compound being detected.

EFFECT OF DOPING ON SELECTIVITY OF SEMICONDUCTOR SENSORS

As noted in the introduction, the main disadvantage of semiconductor sensors is their low detection selectivity. One of the ways to solve this problem is,

apparently, by doping the main matrix of the sensor material with various types of metal oxides. Indeed, at present there are indications of an increase in selectivity when using sensors based on mixed oxides (see, for example, [26, 55, 58]). Thus, in the In_2O_3 system doped with aluminum, the sensory effect decreases sharply in the series formaldehyde, ethanol, acetone, and toluene [55]. This result means that increasing the Fermi level of In_2O_3 nanocrystals during doping with Al^{3+} ions [55] reduces the oxidative activity (A_O) of oxygen centers on the surface of these nanocrystals. Below, the influence of doping agents on the state of the sensory system and its activity in the process of detection is considered in more detail.

Role of Oxidative Activity of Oxygen Centers in Doping

The oxygen centers of the sensory reaction, as mentioned above, are the radical O^- anions chemisorbed on the surface. Oxidative activity is characterized by a constant reaction rate (k) of these radical anions with reducing agents, for example, with formaldehyde:

$$CH_2O + O^- \rightarrow CO + H_2O + e^-. \quad (3)$$

The electron e^- formed in this reaction goes into the conduction band of the semiconductor. The energy gain for such an electron transition depends on the electronic affinity of the semiconductor nanocrystals. The decrease in values k of this reaction and magnitude A_O for In_2O_3 nanocrystals when doped with Al^{3+} ions is due to the decrease in the thermal effect of the reaction as a result of the decrease in the electronic affinity of the nanocrystals due to an increase in the Fermi level.

The oxidative activity of oxygen centers in In_2O_3 nanocrystals doped by Al^{3+} ions decreases so much that they can selectively oxidize only a strong reducing agent (for example, formaldehyde), but react poorly with other, relatively weak reducing agents (for example, ethanol and acetone) [55]. A similar change in the selectivity of the sensor during the detection of the aforementioned series of compounds was found for two-component sensors based on La_2O_3–In_2O_3 [40] and Ga_2O_3–In_2O_3 [59] composites, in which In_2O_3 nanocrystals are doped with La and Ga ions during the formation of the composite.

Interestingly, the increase in the sensory effect as a result of the doping of In_2O_3 nanocrystals still happens, despite the decrease in the oxidative activity of the oxygen centers noted in the works [40, 55, 59]. Probably, in this case, the decrease in the activity of oxygen centers is overlapped by the increase in the reaction rate due to the sharp increase in the number of oxygen centers as a result of the increase in the concentration of chemisorbed oxygen. This indicates the possibility of a targeted effect on the selectivity of a metal oxide sensor by changing its oxidative activity by doping it with metal ions of various electronic structures.

Role of Changes in Adsorption Properties during Doping

Another factor that determines the sensitivity and selectivity of a sensor is the adsorption properties of the sensitive layer [60, 61]. The adsorption of compounds with oxygen-containing functional groups, such as formaldehyde, acetone, and alcohols, depends on the acid-base properties of the sensitive layer. It is known that the first stage in the detection of alcohols by a metal oxide sensor is the catalytic reaction of alcohol molecules with a metal oxide, which can proceed in two directions: through dehydration and oxidative dehydrogenation [62, 63]:

$$C_2H_5OH \rightarrow C_2H_4 + H_2O, \quad (4)$$

$$C_2H_5OH + O^- \rightarrow CH_3CHO + H_2O + e^-. \quad (5)$$

However, only oxidative dehydrogenation leads to a sensory effect (5), since the electrons captured by oxygen return to the conduction band as a result of this reaction. The ratio between the amounts of ethylene and acetaldehyde formed during the catalytic decomposition of alcohol on the surface of nanocrystals, and hence the sensory effect, depend on the acid-base properties of the sensitive layer. These properties can be purposefully changed by doping nanocrystals with metal ions of various electronic structures [62–64].

Investigation of nanostructured sensors based on SnO_2 and In_2O_3 doped with different ions showed that the proportion of acetaldehyde in the primary decay products of ethanol increases with a decrease in electronegativity and an increase in the basicity of the doping ions. Accordingly, the sensory effect when detecting alcohol with doped oxides is enhanced. A particularly significant increase in the sensory effect is observed [63] as a result of the dissolution of La^{3+} ions, whose electronegativity is significantly lower than the electronegativity of tetravalent tin ions [62], in SnO_2 nanocrystals. Substitution of Sn^{4+} ions La^{3+} ions in the SnO_2 lattice increases the basicity of SnO_2 nanocrystals and increases the number of alkaline centers on their surface, which stimulates the adsorption of acid-type compounds such as alcohols and formaldehyde on the surface of these nanocrystals.

Role of Increasing the Concentration of Oxygen Vacancies in Doping

It should be noted that the doping of the crystal sensitive SnO_2 layer by La^{3+} ions not only increases the basicity of the La–SnO_2 layer but also increases the concentration of oxygen vacancies [64], which, as already noted, chemisorb oxygen with the formation of active oxygen centers. Thus, the sharp increase in

the sensory effect when detecting alcohols and aldehydes by SnO_2 nanocrystals doped with La^{3+} ions is the result of the combined action of acid-base and oxidizing factors, which especially strongly increase the sensitivity of this system to formaldehyde [40].

A similar joint sensitizing effect of these factors on the sensory effect in the detection of alcohols and aldehydes is also manifested as a result of the doping of the crystalline layers by the In_2O_3 ions of trivalent yttrium [65]. In this case, an increase in the concentration of formaldehyde chemisorbed by In_2O_3 containing Y^{3+} ($Y–In_2O_3$) ions is consistent with the increase in the Fermi level of $Y–In_2O_3$ nanocrystals under the action of doping yttrium ions [65]. As in [40, 55, 59], the difference between the Fermi level of the sensitive layer and the upper free orbital of chemisorbed oxygen increases. This increases the concentration of chemisorbed oxygen, including the concentration of oxygen active centers involved in the sensory process. Thus, in the $Y–In_2O_3$ sensor system, there is a joint action of acid-base and oxidizing factors, which especially strongly increases the sensitivity of this system to formaldehyde [65].

The results of the study of two-component sensory systems once again show that the sensitization of the sensory effect when activating the ions of another component introduced into the nanocrystal lattice depends on the concentration of the latter. With an increase in the concentration of such ions, the sensory effect first increases, reaches the maximum, the value of which depends on the structure of the nanocrystal lattice, as well as on the size and electronic structure of the intercalated ions, and then decreases with a further increase in their concentration.

Investigation of sensory systems based on oxides such as SnO_2 [35, 66, 67], In_2O_3 [35–37, 68–72], ZnO [73], and Co_3O_4 [70–72, 74] doped with various ions showed that the dependence of the sensory effect on the concentration of different types of doping ions has the same form as the dependence of the amount of chemisorbed oxygen.

Effect of the Position of Doping Ions in the Crystal Lattice

When analyzing the results for mixed metal oxide systems, it should be borne in mind that the transition of ions between components can occur by replacing ions at the nodes of the nanocrystal (doping) or by introducing ions into the interstitial space of the nanocrystal [75, 76]. Thus, during doping with the formation of substitutional solutions, accompanied by a change in the charge of ions or the bonds of metal ions with oxygen in the crystal lattice, conditions are created that favor the appearance of oxygen vacancies and thereby stimulate a sensory response.

The concentration range of the doping agent at which the solution remains stable depends on the structure of the nanocrystal lattice, as well as on the size and valence of the doping ions. With an increase in the concentration of doping ions, the substitutional solutions are partially or completely destroyed with the transition of doping ions from nodes of the lattice to the interstitial space. In this range of concentrations of the "foreign" ions introduced into the nanocrystal, the effect of their amount on the concentration of oxygen vacancies in the metal oxide lattice decreases.

The effect of doping ions on the lattice of nanocrystals can be characterized by studying the stresses in the lattice at various concentrations of these ions. The nature and magnitude of stresses are determined by the Williamson–Hall equation [77]:

$$(\beta/\lambda)\cos\theta = k/D + (4\varepsilon/\lambda)\sin\theta,$$

where k is the coefficient depending on the shape of the particle and equal to 0.9 for spherical particles; D is the size of the nanocrystals; 2θ is the diffraction angle; β is the width of the X-ray peak at half the height of the peak corresponding to the diffraction angle; λ is the wavelength of X-ray radiation; and ε is the magnitude of the voltage induced by lattice defects, including doping ions.

In the work [68], In_2O_3 nanocrystals doped with manganese ions are studied in detail. The slope of the curves constructed in accordance with the Williamson–Hall equation for various concentrations of Mn determines the nature of the stresses in the lattice arising from doping. The negative slope of these curves at Mn ion concentrations below 5% indicates the compression of the nanocrystal lattice due to the formation of Mn substitutional solutions in In_2O_3 [68]. In the system containing 5% manganese, a sharp change in the type of stresses occurs: the compression of the lattice is replaced by its expansion. The substitutional solution remains stable at a manganese concentration below 5%, and at higher Mn concentrations, the solution decomposes, and part of the doping manganese ions pass into the In_2O_3 interstitial space. This leads to a change in voltages. Simultaneously with the rearrangement of the nanoparticle lattice observed at an Mn concentration above 5%, a sharp drop in the sensory effect occurs [68].

Similar phenomena were noted for SnO_2 nanoparticles doped with In ions during their formation on the surface of In_2O_3 nanocrystals [35] or doped with Ni ions during the codeposition of NiO and SnO_2 from a solution of Ni and Sn salts [66]. The results of these studies are in complete agreement with the remarks made above about the relationship between the arrangement of doping ions in the lattice of nanoparticles and the sensory effect.

It should be taken into account that, according to the XPS data, doping ions forming the substitutional solid solution in nanocrystals are inhomogeneously distributed over the entire volume, so that the surface layers of nanocrystals are significantly enriched with

these ions [62]. In particular, in SnO_2 crystals with the average size of about 100 nm, doped with In ions, with the average concentration of such ions in the bulk of the nanocrystal of about 1%, the concentration of the latter in the surface layer exceeds that in the bulk layer by a factor of 4.

Enrichment of the surface layers of a nanocrystalline sensor with doping elements with an increase in their volume concentration (for substitutional solutions of Mn in In_2O_3 over 5%) stimulates the segregation of these elements on the surface of nanocrystals [63]. This prevents the interaction of oxygen and the detected gas with the surface of the sensitive layer and reduces the sensory effect [64]. This circumstance may be another reason for the drop in the sensitivity of the metal oxide sensor, which is mentioned above and is typical for many systems, with an increase in the concentration of doping elements.

THE INFLUENCE OF HETEROGENEOUS CONTACTS ON THE SENSORY EFFECT

As mentioned above, the sensory effect is expressed by a change in the conductivity of the sensitive layer as a result of the reaction of the detected gas with oxygen atoms or molecules chemisorbed on the surface of metal oxide nanoparticles. The conductivity of this layer is determined by the chains of particles in contact with each other and thereby forming paths of current flow between the electrodes of the measuring system. Most of the two-component sensor materials considered in this review are mixtures of randomly located metal oxide nanoparticles of both components. Such mixtures were obtained by the mechanical mixing of nanoparticles (see, for example, [3, 35, 74, 78]) or by the coprecipitation of metal oxides from mixed solutions [49, 59, 62, 63, 78, 79].

At low contents of one of the metal oxide components, the codeposition of metal oxides leads to the formation of a solid solution of this component in nanocrystals of another oxide. As a result, a single-phase system is formed in which the current flows through aggregates of the solid solution's nanoparticles. However, the range of the existence of metastable solid solutions in a two-component metal oxide composite is extremely limited. The solutions decompose with the segregation of individual metal oxides, so that the particles of the solid solution coexist with the particles of the segregated material [76].

In most two-component metal oxides, these components form two phases, and therefore, in accordance with the percolation theory [80], such composites have different paths of current flow, which depend on the composition of the system, as well as the size and nature of the particles of the components. In accordance with the changes in the paths of current flow, the action of the detected gas on the conductivity of the composite changes, which determines the sign and magnitude (increase or decrease in conductivity) of the conductometric sensory effects.

All these issues are discussed in [81] using the percolation model of the conductivity of a material structured on the nanoscale. The conductivity and sensory properties of a completely disordered composite with a random arrangement of TiO_2 nanoparticles related to the two-phase modifications of this oxide—anatase (A) with electronic (n) conductivity and rutile (R) with hole (p) conductivity—are considered. In such a system, there are three types of intercrystalline contacts: A–A, R–R, and A–R; moreover, an internal electric field is formed in the heterogeneous A–R contacts caused by the transfer of electrons from R to A, since crystals A differ from crystals R by a higher electron affinity [82]. This field in a disordered system can increase the conduction barrier. Based on this, the authors of [81] conclude that, in two-phase composites, two parallel mutually exclusive conduction paths are most probable: through the homogeneous contacts of nanoparticles n–n or p–p, in this case, along the chains of nanoparticles A or R. The nanoparticles of the second component, which are not included in the conduction path, are modifiers, interaction with which changes the chemical and electronic characteristics of the conducting nanocrystals.

A similar approach can be used when considering two-phase structures based on n-nanocrystals K1 and K2 with a different work function of the electron: W_{e1} and W_{e2}. In this case, with a random arrangement of nanocrystals, the heterogeneous contacts K1–K2, as in the composite consisting of n- and p-nanoparticles, increase obstacles in the path of the current, so that the current in the system flows, bypassing these contacts, along homogeneous paths through the K1–K1 or K2–K2 contacts. Such systems are, in particular, ZnO–In_2O_3 nanocomposites obtained from mixtures of In_2O_3 powder with ZnO powder as a result of grinding them with the addition of water or alcohol [79].

In binary ZnO–In_2O_3 systems with the zinc oxide (X_{Zn}) content less than 3 wt %, ZnO dissolves in In_2O_3 crystals, as a result of which a homogeneous conglomerate of In_2O_3modified with Zn^{2+} ions is formed [18, 19]. The increase in the resistance and sensory response during the detection of hydrogen and carbon monoxide in this case is explained by the dissolution of In_2O_3 ions of lower valence in the lattice, which leads to the formation of additional oxygen vacancies in the In_2O_3 nanoparticles.

With a further increase in the ZnO content, a composite is formed in which the modified In_2O_3 crystals come into contact with the ZnO crystals. The influence of such contacts on the resistance and sensory properties of the nanocomposite is determined by two factors: chemical and electronic [10].

The formation of oxygen centers O^- of the sensory reaction occurs during the dissociation of chemisorbed

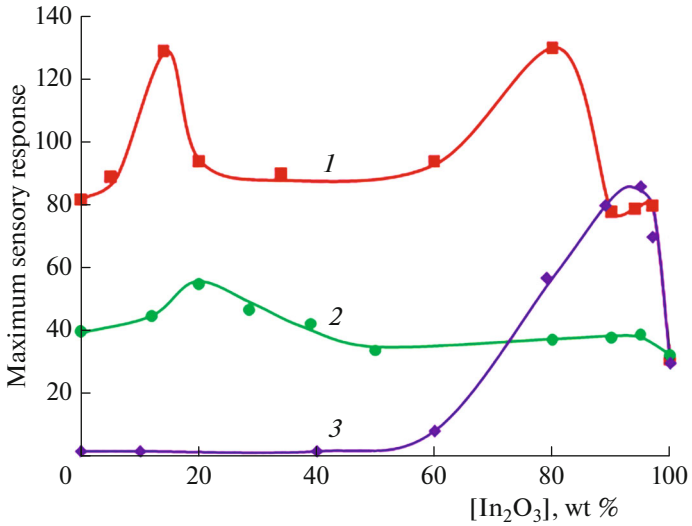

Fig. 1. Effect of the composition of nanoscale structured $ZnO–In_2O_3$ (*1*), $SnO_2–In_2O_3$ (*2*), and $CeO_2–In_2O_3$ (*3*) composites on their maximum sensory response (R_{H_2}/R_0) when detecting 2% H_2 [18–20, 78].

oxygen on the surface oxygen vacancies of a metal oxide nanoparticle [43]. ZnO nanoparticles have high catalytic activity [83]. At the same time, the catalytic activity of In_2O_3 nanoparticles is much lower [84]. Therefore, in $ZnO–In_2O_3$ composites, the oxygen dissociation with the formation of chemisorbed oxygen atoms occurs predominantly on the surface of ZnO nanoparticles [85], but the current in these composites at $X_{Zn} < 80\%$ flows through aggregates of the electron-rich In_2O_3 nanoparticles [19].

At the contacts of the In_2O_3 and ZnO nanoparticles, the oxygen atoms formed on the surface of the ZnO nanoparticles are transferred to the surface of the In_2O_3 nanoparticles (spillover) [86], capturing the conduction electrons and transforming into O^- radical anions chemisorbed on the surface of the In_2O_3 nanoparticles. These radical anions are involved in the detection reaction of reducing compounds, in particular CO and H_2. Thus, the ZnO nanoparticles perform the chemical sensitization of the sensory effect in the $ZnO–In_2O_3$ composite in accordance with the definition given in [10].

Chemical sensitization of the process is most effective in the composite when the conducting aggregates In_2O_3 come into contact with the ZnO nanocrystals along the entire current path. For In_2O_3 and ZnO nanocrystals of approximately the same size, such aggregates appear when the ZnO content is about 20 wt %, which corresponds to the maximum sensory response (Fig. 1, curves *1* and *2*) [19].

A further increase in the ZnO content in the composite probably decreases the number of conducting filaments of In_2O_3 particles related to the ZnO particles due to the fact that these filaments are broken by the ZnO inclusions. Accordingly, the sensitization of the sensor effect in the composite performed by ZnO nanoparticles decreases. Chemical sensitization of the sensor effect is also observed in composites obtained by mixing the In_2O_3 and CeO_2 nanoparticles. In these systems, the current also flows through aggregates of In_2O_3 nanoparticles, while the CeO_2 nanoparticles, like the ZnO nanoparticles, act as catalysts for the dissociation of oxygen molecules with the subsequent transfer of the oxygen atoms to the In_2O_3 nanoparticles (Fig. 1, curve *3*) [20, 78]. Shift of the maximum of the sensory sensitivity of the $CeO_2–In_2O_3$ composite to the region of lower (in comparison with the $ZnO–In_2O_3$) concentrations of CeO_2 can be explained by the fact that the CeO_2 nanoparticles in composites with In_2O_3 studied in [20, 78] are much smaller than ZnO nanoparticles.

Unlike the $ZnO–In_2O_3$ composite, in the $SnO_2–In_2O_3$ composite, when hydrogen is detected, there is practically no chemical sensitization of the sensor effect by the SnO_2 nanoparticles [18, 19]. This difference between the indicated composites can be explained by the fact that the catalytic activity of the SnO_2 nanoparticles in the processes of the dissociative chemisorption of oxygen and hydrogen is much lower than that of the ZnO nanoparticles.

At the same time, a significant increase in the sensory effect upon modification of indium oxide with additions of ZnO and SnO_2 caused by more intense chemisorption of oxygen on the surface of the composite was observed during the detection of formaldehyde [87, 88]. This indicates the dependence of the sensitization of the sensory effect not only on the cat-

alytic dissociation of oxygen but also on the reactivity of the detected compounds.

When decreasing X_{In} up to 20–30 wt % in accordance with the percolation model in the SnO_2–In_2O_3 and ZnO–In_2O_3 composites, the path of the current flow changes from the conductive aggregates of In_2O_3 nanoparticles to the conductive aggregates of SnO_2 and ZnO nanoparticles [18, 19]. In a composite with conductivity through these aggregates, when hydrogen is detected, electronic sensitization of the sensor effect is manifested due to the transfer of electrons from the In_2O_3 particles to the SnO_2 and ZnO particles with a higher electron affinity, since the degree of electron transfer as a result of the sensory process increases [18]. In [89], the role of chemical and electronic sensitization by gold nanoparticles on the detection of acetone, toluene, ammonia, and hydrogen sulfide by metal oxide composites based on WO_3, SnO_2, and NiO is also analyzed in detail.

Methane detection by nanoscale-structured sensors consisting of electron-rich In_2O_3 nanocrystals of the *n*-type of about 1 μm, coated with catalytically active Ni_2O_3 nanoclusters of the *p*-type with a size of about 10 nm, is studied in [90]. In this system, in contrast to the nanocomposites described above, there are conducting paths of only one type of In_2O_3 particles of the *n*-type, modified as a result of contacts with Ni_2O_3 nanoclusters of the *p*-type. The authors of [90] believe that the observed increase in the sensory effect is explained by the significant drop in conductivity caused by these contacts. In our opinion, a more important reason The increase in the concentration of the active centers of the sensory reaction—O^- anion radicals—as a result of the chemisorption and dissociation of oxygen molecules on the surface of the catalytically active Ni_2O_3 nanoclusters. Then oxygen atoms are transferred to the surface of the In_2O_3 particles, accompanied by the capture of conduction electrons by these atoms of the In_2O_3 nanoparticles.

Coating In_2O_3 particles by Ni_2O_3 clusters leads not only to an increase in the sensory effect but also to a decrease in the temperature of methane detection [90]. Composites consisting of In_2O_3 fibers containing SnO_2 nanoclusters on the surface [91] behave similarly. Nanoscale In_2O_3 fibers were formed by the method of electrospinning, and the clusters were formed by impregnating the fibers with a tin salt solution, followed by its hydrolysis and the formation of SnO_2. In this system (in contrast to the SnO_2–In_2O_3 nanocomposites discussed above), the SnO_2 nanoclusters are in an active metastable state [91]. The dissociative chemisorption of oxygen proceeding on their surface and the adsorption of oxygen atoms formed in this case on the In_2O_3 fibers lead to the formation of active O^- centers in the SnO_2–In_2O_3 boundary layers. This not only enhances the sensory effect of detecting ethanol in air but also reduces the return time of the sensitive layer of the sensor—the surface of the In_2O_3 fibers—to the initial state, since under the action of SnO_2 clusters the rate of deposition of oxygen atoms on the fiber surface increases after the removal of ethanol vapors [91].

In the work [78], nanocomposites consisting of In_2O_3 or SnO_2 nanocrystals containing clusters of CeO_2 of 6 to 8 nm were studied. These clusters (as well as SnO_2 and ZnO, see Fig. 1) in the composite with In_2O_3 nanocrystals lead to an increase in the sensory effect when detecting hydrogen. At the same time, in the composite based on SnO_2 nanocrystals, additives of cerium oxide sharply reduce the sensory effect [78].

The structure of In_2O_3 nanocrystals during the formation of CeO_2–In_2O_3 composites barely changes [78]. An increase in the sensory effect in this composite, as in other similar systems, is due to the catalytic dissociation of the oxygen chemisorbed on the CeO_2 clusters with the subsequent transfer of oxygen atoms to the surface of In_2O_3 nanocrystals, which is accompanied by the capture of electrons by these atoms from the conduction band. As a result of the reaction

$$H_2\,(\text{ads}) + O^- \rightarrow H_2O + e^- \qquad (6)$$

the e^- electrons captured by oxygen are freed.

It should be noted that the addition of CeO_2 leads not only to an increase in the sensory activity of indium oxide structured at the nanoscale but also to a decrease in the operating temperature during the detection of reducing gases [92]. The increased sensory activity of In_2O_3 with the addition of CeO_2 was found also with the detection of ethanol [93].

In the CeO_2–SnO_2 composite, the picture of the sensory process is most likely basically the same. The difference from the CeO_2–In_2O_3 composite lies in the fact that, as the XPS data and the temperature dependence of the conductivity of the CeO_2–SnO_2 composite show [78], the structure of SnO_2 nanocrystals, at least the structure of their surface layers, which determines the conductive and sensory properties of composites, is modified by the action of the cerium ions dissolved in these layers. The replacement of Sn ions by Ce ions in the SnO_2 lattice leads to a weakening of the Sn–O bonds [94]. Accordingly, the binding energy of electrons with the surrounding ions in oxygen SnO_2 vacancies should increase, as a result of which the activation energy of conduction increases [78].

The oxygen atoms passing from CeO_2 clusters on the surface of In_2O_3 and SnO_2 nanoparticles are localized on the surface defects of nanoparticles (mainly oxygen vacancies), as noted in the form of O^-. In this case, as a result of the O^- reaction with a reducing agent, in particular with H_2 (see reaction (5)), first, most likely, an intermediate complex of an electron with a vacancy (electron trap) is formed, which then

decays with the transition of the electron to the conduction band of the semiconductor. The formation of deep electronic traps in the CeO_2–SnO_2 composite prevents this transition and thus can reduce the sensory effect.

The decrease in sensitivity when hydrogen is detected by a CeO_2–SnO_2 composite sensor compared to an SnO_2-sensor was also established in [95]. At the same time, the crystalline composite CeO_2–SnO_2 nanosized fibers formed by the method of electrospinning when detecting alcohol also show a higher sensory effect than similar fibers from SnO_2 obtained by the same method [96]. When detecting alcohol, it is necessary to take into account the possible increase in its adsorption by nanoparticles of the composite in comparison with the adsorption by SnO_2 nanocrystals due to the intercharging of composite nanoparticles as a result of the transfer of electrons from CeO_2 particles (the work function of an electron is 4.6 eV [97]) to SnO_2 particles (the work function of an electron is 4.9 eV [98]) and, as a consequence, the formation of new dipole adsorption centers.

CONCLUSIONS

Experimental and theoretical works devoted to the study of the structure, conductivity, and sensory properties of metal oxide systems structured on the nanoscale are considered and analyzed. The sensitivity and selectivity of conductometric sensors are improved by using multicomponent composite systems that combine metal oxides with different electronic characteristics and chemical properties. The sensory effect in the detection of reducing gases is determined by the chemisorption of oxygen and the detected gas on metal oxide particles and the reaction of chemisorbed molecules of the detected gas with oxygen ions. As a result, the conductivity of the sensitive layer changes. For efficient operation, sensor systems must contain both catalytically active nanoclusters and nanoparticles with a high concentration of conduction electrons.

The main mechanisms of the interaction of nanoparticles include catalytic reactions on the surface of one of the components, the transfer of reaction products to another, and the effect of these products on the electronic subsystem of the latter. We need to take into account the capture of electrons from the bulk of nanoparticles by the adsorbed oxygen atoms and the further return of an electron to the conduction band during the reaction of O^- with molecules of the detected gas. An important role in increasing the sensory activity of mixed systems during their formation is played by the movement of metal ions of one oxide into nanoobjects of another component. The structure and properties of nanoparticles change upon iso- and heterovalent doping. In this case, not only is the charge important but also the ratio of the sizes of the replaced and incorporated ions. This study showed that the sensitization of the sensor effect upon the incorporation of activating ions of another component into the nanocrystal lattice depends not only on the charge and size but also on the concentration of the incorporated ions.

Depending on the content of the second component, the composite can exist in the form of a single-phase system in which the current flows through aggregates of the nanoparticles of a solid solution or form two phases. In the latter case, in composites, there are different paths of current flow, which depend on the composition of the system, as well as the size and type of particles of the components. In such systems, the conductivity of the composite is greatly influenced by the interaction of heterogeneous contacts of dissimilar oxides.

FUNDING

This study was supported by the Russian Foundation for Basic Research (project no. 20-13-50055).

OPEN ACCESS

This article is licensed under a Creative Commons Attribution 4.0 International License, which permits use, sharing, adaptation, distribution and reproduction in any medium or format, as long as you give appropriate credit to the original author(s) and the source, provide a link to the Creative Commons license, and indicate if changes were made. The images or other third party material in this article are included in the article's Creative Commons license, unless indicated otherwise in a credit line to the material. If material is not included in the article's Creative Commons license and your intended use is not permitted by statutory regulation or exceeds the permitted use, you will need to obtain permission directly from the copyright holder. To view a copy of this license, visit http://creativecommons.org/licenses/by/4.0/.

REFERENCES

1. I. D. Kim, A. Rothschild, and H. L. Tuller, Acta Mater. **61**, 974 (2013).
2. E. Comini, Anal. Chim. Acta **568**, 28 (2006).
3. Md. A. Al. Mamun and M. R. Yuce, Adv. Funct. Mater. **30**, 2005703 (2020).
4. K. Sahner and H. L. Tuller, J. Electroceram. **24**, 177 (2010).
5. N. Taguchi, US Patent No. 3.631.436 (1971).
6. R. B. Vasiliev, L. I. Ryabova, M. N. Rumyantseva, and A. M. Gaskov, Russ. Chem. Rev. **73**, 939 (2004).
7. D. R. Miller, S. A. Akbar, and P. A. Morris, Sens. Actuators, B **204**, 250 (2014).
8. N. Barsan and U. Weimar, J. Electroceram. **7**, 143 (2001).
9. G. Korotcenkov, Mater. Sci. Eng. B **139**, 1 (2007).
10. N. Yamazoe, Y. Kurorawa, and T. Seiyama, Sens. Actuators, B **4**, 283 (1983).

11. M. N. Rumyantseva, V. A. Kovalenko, A. M. Gas'kov, and T. Pagnier, Ross. Khim. Zh. **51**, 61 (2007).
12. G. N. Gerasimov, V. F. Gromov, O. J. Ilegbusi, and L. I. Trakhtenberg, Sens. Actuators, B **240**, 613 (2017).
13. G. Korotcenkov and B. K. Cho, Sens. Actuators, B **244**, 182 (2017).
14. A. Schwarz, C. Contescu, and A. Contescu, Chem. Rev. **95**, 477 (1995).
15. V. V. Krivetskii, A. Ponzoni, E. Comini, S. M. Badalyan, M. N. Rumyantseva, and A. M. Gaskov, Inorg. Mater. **46**, 1100 (2010).
16. G. Korotcenkov, I. Boris, A. Cornet, et al., Sens. Actuators, B **120**, 657 (2007).
17. C.-Yu. Lin, Yu.-Yu. Fang, Ch.-W. Lin, J. J. Tunney, and K.-C. Ho, Sens. Actuators, B **146**, 28 (2010).
18. L. I. Trakhtenberg, G. N. Gerasimov, V. F. Gromov, T. V. Belysheva, and O. J. Ilegbusi, Sens. Actuators, B **169**, 32 (2012).
19. L. I. Trakhtenberg, G. N. Gerasimov, V. F. Gromov, T. V. Belysheva, and O. J. Ilegbusi, Sens. Actuators, B **187**, 514 (2013).
20. L. I. Trakhtenberg, G. N. Gerasimov, V. F. Gromov, T. V. Belysheva, and O. J. Ilegbusi, Sens. Actuators, B **209**, 562 (2015).
21. S. K. Poznyak, D. V. Talapin, and A. I. Kulak, J. Phys. Chem. B **105**, 4816 (2001).
22. D.-W. Kim, I.-S. Hwang, S. J. Kwon, et al., Nano Lett. **7**, 3041 (2007).
23. T. V. Belysheva, G. N. Gerasimov, V. F. Gromov, E. Yu. Spiridonova, and L. I. Trakhtenberg, Russ. J. Phys. Chem. A **84**, 1554 (2010).
24. W. J. Moon, J. H. Yu, and C. G. Man, Sens. Actuators, B **87**, 464 (2002).
25. J. Tamaki, K. Moriya, N. Miura, and N. Yamazoe, J. Electrochem. Soc. **144**, L158 (1997).
26. N. Yamazoe, Sens. Actuators, B **5**, 7 (1991).
27. N. Yamazoe and K. Shimanoe, J. Sensors **138**, 1 (2009).
28. E. L. Nagaev, Sov. Phys. Usp. **35**, 747 (1992).
29. L. I. Trakhtenberg, G. N. Gerasimov, E. I. Grigoriev, et al., *Studies in Surface Science and Catalysis* (Elsevier, Amsterdam, 2000).
30. B. V. Lidskii, I. I. Oleynik, V. S. Posvyanskii, and L. I. Trakhtenberg, J. Phys. Chem. C **119**, 16286 (2015).
31. K. S. Kurmangaleev, M. I. Ikim, M. A. Kozhushner, and L. I. Trakhtenberg, Appl. Surf. Sci. **546**, 149011 (2021).
32. M. A. Kozhushner, L. I. Trakhtenberg, A. C. Landerville, and I. I. Oleynik, J. Phys. Chem. C **117**, 11562 (2013).
33. M. A. Kozhushner, L. I. Trakhtenberg, V. L. Bodneva, et al., J. Phys. Chem. C **118**, 11444 (2014).
34. V. L. Bodneva, M. A. Kozhushner, V. S. Posvyanskii, and L. I. Trakhtenberg, Russ. J. Phys. Chem. B **13**, 190 (2019).
35. G. N. Gerasimov, V. F. Gromov, M. I. Ikim, et al., Sens. Actuators, B **320**, 128406 (2020).
36. J. Shen, F. Li, B. Yin, et al., Sens. Actuators, B **253**, 461 (2017).
37. X. Zhu, Y. Li, H. Zhang, et al., J. Alloys Compd. **830**, 154578 (2020).
38. K. Sakthiraj and K. Balachandrakumar, J. Magn. Magn. Mater. **395**, 205 (2015).
39. D. Wei, W. Jiang, H. Gao, et al., Sens. Actuators, B **276**, 413 (2018).
40. X. Zeng, L. Liu, Y. Lv, et al., Chem. Phys. Lett. **746**, 137289 (2020).
41. S. C. S. Lemos, E. Nossol, J. L. Ferrari, et al., Inorg. Chem. **58**, 11738 (2019).
42. V. D. Kapse, S. A. Ghosh, F. C. Raghuwanshi, and S. D. Kapse, Sens. Actuators, B **137**, 681 (2009).
43. B. Slater, C. R. A. Catlow, D. E. Williams, and A. M. Stoneham, Chem. Commun., No. 14, 1235 (2000).
44. W. Zeng, Y. Li, B. Miao, L. Lin, and Z. Wang, Sens. Actuators, B **191**, 1 (2014).
45. C. Zhong, Z. Lin, F. Guo, and X. Wang, J. Nanosci. Nanotechnol. **15**, 4296 (2015).
46. J. Maier and W. Göpel, J. Solid State Chem. **72**, 293 (1988).
47. G. N. Gerasimov, V. F. Gromov, M. I. Ikim, E. Yu. Spiridonova, M. M. Grekhov and L. I. Trakhtenberg, Russ. J. Phys. Chem. B **13**, 763 (2019).
48. J. Liu, X. Liu, Z. Zhai, et al., Sens. Actuators, B **220**, 1354 (2015).
49. W. S. Epling, C. H. F. Peden, M. A. Henderson, and U. Diebold, Surf. Sci. **412–413,** 333 (1998).
50. J. Sun, G. Yin, T. Cai, et al., RSC Adv. **8**, 33080 (2018).
51. G. Korotcenkov, I. Boris, V. Brinzari, S. H. Han, and B. K. Cho, Sens. Actuators, B **182**, 112 (2013).
52. Q. Zhou, W. Chen, L. Xu, et al., Ceram. Int. **44**, 4392 (2018).
53. K. Bunpang, A. Wisitsoraat, A. Tuantranont, et al., Sens. Actuators, B **291**, 177 (2018).
54. Z. Jiang, R. Zhao, B. Sun, et al., Ceram. Int. **42**, 15881 (2016).
55. H. Chen, Y. Zhao, L. Shi, et al., ACS Appl. Mater. Interfaces **35**, 29795 (2018).
56. M. T. Greiner, L. Chai, M. G. Helander, W.-M. Tang, and Z.-H. Lu, Adv. Funct. Mater. **22**, 4557 (2012).
57. C. A. Pan and T. P. Ma, Appl. Phys. Lett. **37**, 714 (1980).
58. S. A. Vladimirova, M. N. Rumyantseva, D. G. Filatova, et al., J. Alloys Compd. **721**, 249 (2017).
59. T. Wang, B. Jiang, Q. Yu, et al., ACS Appl. Mater. Interfaces **11**, 9600 (2019).
60. V. V. Krivetskiy, M. N. Rumyantseva, and A. M. Gaskov, Russ. Chem. Rev. **82**, 917 (2013).
61. M. V. Grishin, A. K. Gatin, S. Yu. Sarvadii, V. G. Slutskii, B. R. Shub, A. I. Kulak, T. N. Rostovshchikova, S. A. Gurevich, V. M. Kozhevin, and D. A. Yavsin, Russ. J. Phys. Chem. B **14**, 697 (2020). https://doi.org/10.1134/S1990793120040065
62. T. Jinkawa, G. Sakai, J. Tamaki, N. Miura, and N. Yamazoe, J. Mol. Catal. A: Chem. **155**, 193 (2000).
63. V. V. Krivetskiy, R. V. Rozhik, M. N. Rumyantseva, N. E. Mordvinova, A. V. Smirnov, A. V. Garshev, and A. M. Gaskov, Russ. J. Inorg. Chem. **61**, 1368 (2016).
64. Y. Chen, Z. Dong, X. Xue, et al., Appl. Phys. A **126**, 299 (2000).

65. Y. Zhao, X. Zou, H. Chen, X. Chu, and G.-D. Li, Inorg. Chem. Front. **6**, 1767 (2019).
66. Z. Li and J. Yi, Sens. Actuators, B **243**, 96 (2017).
67. J. Sun, G. Yin, T. Cai, et al., RSC Adv. **8**, 33080 (2018).
68. K. Anand, J. Kaur, and R. C. Singh, Ceram. Int. **42**, 10957 (2016).
69. J. Hu, Y. Sun, Y. Xue, et al., Sens. Actuators, B **257**, 124 (2018).
70. H. Yamaura, K. Moriya, N. Miura, and N. Yamazoe, Sens. Actuators, B **65**, 39 (2000).
71. M. I. Ikim, G. N. Gerasimov, V. F. Gromov, T. V. Belysheva, E. Yu. Spiridonova, I. V. Shapochkina, R. A. Alizade, and L. I. Trakhtenberg, Russ. J. Phys. Chem. B **11**, 846 (2017).
72. V. F. Gromov, G. N. Gerasimov, T. V. Belysheva, M. I. Ikim, E. Yu. Spiridonova, M. M. Grekhov, R. A. Ali-zade, and L. I. Trakhtenberg, Russ. J. Phys. Chem. B **12**, 129 (2018).
73. T. V. Belysheva, E. Yu. Spiridonova, M. I. Ikim, G. N. Gerasimov, V. F. Gromov, and L. I. Trakhtenberg, Russ. J. Phys. Chem. B **14**, 298 (2020).
74. F. Qu, N. Zhang, D. Liu, et al., Sens. Actuators, B **308**, 127651 (2020).
75. F. H. Aragon, J. A. H. Coaquira, L. Villegas-Lelovsky, et al., J. Phys.: Condens. Matter **27**, 095301 (2015).
76. F. H. Aragon, J. A. H. Coaquira, P. Hidalgo, et al., J. Raman Spectrosc. **42**, 1081 (2011).
77. V. D. Mote, Y. Purushotham, and B. N. Dole, J. Theor. Appl. Phys. **6**, 6 (2012).
78. G. N. Gerasimov, V. F. Gromov, M. I. Ikim, O. J. Ilegbusi, and L. I. Trakhtenberg, Sens. Actuators, B **279**, 22 (2019).
79. B. P. J. de Lacy Costello, R. J. Ewen, N. M. Ratcliffe, and P. S. Sivanand, Sens. Actuators, B **92**, 159 (2013).
80. A. L. Efros, *Physics and Geometry of Disorder: Percolation Theory* (Mir, Moscow, 1987).
81. N. Savage, B. Chwieroth, A. Ginwalla, et al., Sens. Actuators, B **79**, 17 (2001).
82. G. Xiong, R. Shao, T. C. Droubay, et al., Adv. Funct. Mater. **17**, 2133 (2007).
83. S. Polarz, J. Strunk, V. Ischenko, et al., Angew. Chem., Int. Ed. **45**, 2965 (2006).
84. I. Tanaka, M. Mizuno, and H. Adachi, Phys. Rev. B **56**, 3536 (1997).
85. W. Göpel, G. Rocker, and R. Feierabend, Phys. Rev. B **28**, 3427 (1983).
86. A. Kolmakov, D. O. Klenov, Y. Lilach, S. Stemmer, and M. Moskovits, Nano Lett. **5**, 667 (2005).
87. L. Ma, H. Fan, H. Nian, J. Fang, and X. Qian, Sens. Actuators, B **222**, 508 (2016).
88. H. Du, J. Wang, M. Su, et al., Sens. Actuators, B **166–167,** 746 (2012).
89. J. Lee, Y. Jung, S.-H. Sung, et al., J. Mater. Chem. A **9**, 1159 (2021).
90. N. M. Vuong, N. M. Hieu, D. Kim, B. Il. Choi, and M. Kim, Appl. Surf. Sci. **317**, 765 (2014).
91. H. Shen, L. Li, and D. Xu, RSC Adv. **7**, 33098 (2017).
92. X. Liu, L. Jang, X. Jang, et al., Appl. Surf. Sci. **428**, 478 (2018).
93. X. Chen, N. Deng, X. Zhang, et al., J. Nanopart. Res. **21**, 77 (2019).
94. A. Gupta, A. Kumar, M. S. Hegde, and U. V. Waghmare, J. Chem. Phys. **132**, 194702 (2010).
95. C. Li, Z. Yu, S. Fang, et al., J. Phys.: Conf. Ser. **152**, 012033 (2009).
96. W. Qin, L. Xu, J. Song, R. Xing, and H. Song, Sens. Actuators, B **185**, 231 (2013).
97. S. S. Warule, N. S. Chaudhari, B. B. Kale, et al., J. Mater. Chem. **22**, 8887 (2012).
98. M. N. Islam and M. O. Hakim, J. Mater. Sci. Lett. **5**, 63 (1986).